ACS APPLIED ENGINEERING MATERIALS

pubs.acs.org/acsaenm

Article

Additive Manufacturing of a Portable Electrochemical Sensor with a Recycled Conductive Filament for the Detection of Atropine in Spiked Drink Samples

Iana V. S. Arantes, Robert D. Crapnell, Matthew J. Whittingham, Evelyn Sigley, Thiago R.L.C. Paixão, and Craig E. Banks*

Cite This: *ACS Appl. Eng. Mater.* 2023, 1, 2397−2406

Read Online

ACCESS | Metrics & More | Article Recommendations | Supporting Information

ABSTRACT: Additive manufacturing (three-dimensional (3D) printing) has promising features for fast prototyping electrochemical systems, from cells to sensors. Conductive filaments containing carbon black and poly(lactic acid) (CB/PLA) for electrode fabrication are commercially available but usually rely on low carbon content, resulting in poor electrochemical properties. Filament fabrication can be done within the laboratory by exploring different materials according to the desired applications. In this work, recycled PLA was used as the thermoplastic base polymer, alongside CB as the conductive filler, and tris (2-ethylhexyl) trimellitate was introduced into the filament matrix as a plasticizer (CB/PLA/TTM) to fabricate additively manufactured electrodes (AMEs). This enhanced the electrochemical properties toward different redox probes and the forensic target atropine. Thermogravimetric analysis (TGA), scanning electron microscopy (SEM), and X-ray photoelectron spectroscopy (XPS) were used to characterize the filament and AMEs before and after activation. Additive manufacturing has also been used to develop different cell configurations, which is equally important for good electroanalytical performance. Flow analytical techniques, such as batch-injection analysis (BIA), can be used as an alternative to stationary measurements to enhancing sensitivity and detection limits (LOD) via increasing the mass transport of analytes to the electrochemical platform surface, providing automation and high sample throughput. In this context, we developed a compact (∼5 mL capacity) and versatile additively manufactured BIA cell that can either perform static or hydrodynamic analyses by simply placing a lid on the device with a hole for the BIA pipette tip. Moreover, knowing that forensic chemistry necessitates portable analytical tools to help police investigation at the crime scene, the AM-BIA cell and the bespoke AMEs were coupled to a portable electrochemical apparatus for on-site atropine analysis in adulterated beverage samples. Atropine determination was performed by differential pulse voltammetry (DPV) and amperometry (BIA-AMP) in the same cell, presenting good repeatability for both methods (6% RSD). As expected, the BIA-AMP method showed higher sensitivity (0.0783 μA μM^{-1}) and lower LOD (0.51 μM) compared to the stationary DPV method (sensitivity: 0.0148 μA μmol^{-1} L; LOD: 2.60 μM); they both presented good recovery values, varying from 102 to 109% for two spiked samples of gin and whisky. Thus, the versatility and portability of the developed AM-BIA cell coupled with the bespoke filament CB/PLA/TTM allow for rapid and accurate screening and quantification of atropine in real forensic scenarios.

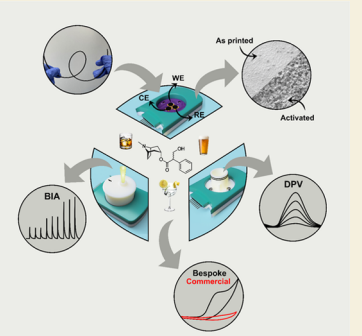

KEYWORDS: *additive manufacturing (3D printing), recycling, electrochemistry, batch-injection analysis, atropine, forensic analysis*

1. INTRODUCTION

Atropine is a medicinal alkaloid isolated from plants of the Solanaceae family but yet, despite its many medical benefits, atropine can be considered both life-saving and life-threatening, as it is extremely dose-dependent. Atropine and other alkaloids are common in illegal practices, such as adulterating drinks aimed at poisoning or carrying out nonconsensual practices with the victim. One well-known case of atropine poisoning was reported in the 1990s when Dr. Paul Agutter contaminated, not just one, but several bottles of tonic water from a local supermarket in an attempt to kill his wife while covering up the crime. This practice usually occurs in bitter-taste drinks, such as gin and tonic, to mask the taste of the drug and increase the chances of success in the crime. Thus, the identification and quantification of this alkaloid are of utmost relevance for clinical and forensic interests.[1,2]

Analytical techniques for atropine determination include separation techniques, such as liquid chromatography, which provide great sensitivity and selectivity but are usually

Received: June 23, 2023
Revised: August 5, 2023
Accepted: August 15, 2023
Published: September 7, 2023

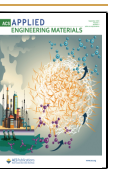

expensive and unsuitable for on-site applications. On the other hand, colorimetric tests can offer portable and low-cost analysis, but they are often not viable for decision-making, serving only as a preliminary test, resulting in false positives due to lack of selectivity.[2] In this context, electrochemical methods can overcome these drawbacks by offering versatile, cheap, and portable sensors, meeting the needs of the police for field analysis.[3−6]

Additive manufacturing (AM) has been widely used along with electrochemical techniques due to the possibility of printing customized cells on demand, in addition to the use of conductive filaments for additively manufactured electrodes (AMEs) fabrication, allowing fully printed lab-on-a-chip devices.[7−9] Poly(lactic acid) (PLA) is typically used as the polymer with carbon black (CB) as the conductive filler. However, the production of bespoke filaments is becoming a trend in AM electrochemistry since using recycled polymers can improve sustainability and reduce production costs.[10] The addition of greater amounts of conductive materials can improve the sensor's performance compared to the commercially available CB/PLA filaments. Plasticizers are added to achieve these high loadings of conductive filler while maintaining adequate low-temperature flexibility of the filament. These compounds can also cause the resultant AME to perform differently. Poly(ethylene succinate) has been reported previously to work well for the production of electroanalytical sensors, whereas poly(ethylene glycol) has been used for energy storage applications.[10,11]

Although the electroanalytical performance of a system strongly depends on the electrode material, the cell configuration and technique used are also equally important. Flow analytical techniques comprising flow and batch-injection analysis can be utilized as an alternative to stationary measurements to increase the mass transport of analytes to the electrode surface, leading to high sensitivity and low detection limits.[12] In short, batch-injection analysis involves sample injection using a micropipette tip directly onto the detector surface under controlled conditions. This approach allows for automated and high sample-throughput analyses.[13,14]

Reports of AM-batch-injection analysis (AM-BIA) cells coupled to AMEs are found in the literature for different applications, including drug detection.[15,16] These cells usually have a high internal volume (∼100 mL), which is undesirable for practical applications due to increased fluid handling and waste generation. Moreover, most works only demonstrate the AM working electrode fabrication using external reference and counter electrodes, hindering the system setup and increasing the cost. Hence, in this paper, we use mixed AM to fabricate a miniaturized and versatile BIA cell capable of performing static and flow analysis for atropine detection in spiked drink samples. Furthermore, a recycled PLA conductive filament containing carbon black and tris (2-ethylhexyl) trimellitate (TTM) as the plasticizer was used to fabricate all three electrodes. Both AM-BIA cell and the bespoke AMEs were estimated at a material cost of £2.53 and attached to a portable electrochemical apparatus, enabling low-cost and on-site analysis of forensic samples.

2. EXPERIMENTAL SECTION

2.1. Chemicals

All chemicals used were of analytical grade and used as received without any further purification. All solutions used deionized water of resistivity not less than 18.2 MΩ·cm (Milli-Q Integral 3 system, Millipore U.K.). Hexaammineruthenium(III) chloride (98%), potassium ferricyanide(III) (99%), potassium hexacyanoferrate(II) trihydrate (98.5−102.0%), dopamine hydrochloride (>99+%), sodium hydroxide (NaOH, >98%), potassium chloride (KCl, 99.0−100.5%), acetic acid (>99%), and phosphate buffered saline (PBS) tablets were purchased from Merck (Gillingham, U.K.). Phosphoric acid (85%), boric acid (>99+%), and carbon black (CB, Super P, >99+%) were purchased from Fisher Scientific (Loughborough, U.K.). Tris(2-ethylhexyl) trimellitate (TTM, >97%) and atropine sulfate monohydrate (>99%) were purchased from TCI chemicals (Oxford, U.K.). Recycled poly(lactic acid) (rPLA) was obtained from Gianeco (Italy). Commercial conductive PLA/carbon black filament with a size of 1.75 mm, ProtoPasta, Vancouver, Canada, was purchased from the U.K. Commercial nonconductive PLA filament with a size of 1.75 mm, galaxy silver, was purchased from Prusa Research (Prague, Czech Republic).

Atropine standard stock solutions were prepared by dissolution in deionized water. The Britton−Robinson (BR) buffer solution was prepared from a mixture of 0.04 mol L^{-1} acetic acid, boric acid, and phosphoric acid. The pH, from pH 2.0 to 12.0, was adjusted using 1.0 mol L^{-1} NaOH.

2.2. Recycled Filament Production

All rPLA were dried in an oven (60 °C/2.5 h) in order to eliminate any residual water in the polymer. The polymer composition utilized 65 wt % rPLA, 10 wt % tris(2-ethylhexyl) trimellitate (TTM), and 25 wt % CB, which were mixed at 170 °C with Banbury rotors at 70 rpm for 5 min using a Thermo-Haake Poydrive dynameter fitted with a Thermo-Haake Rheomix 600 (Thermo-Haake, Germany). The polymer composite was allowed to reduce down to room temperature before being granulated further. The sample was collected and processed through the hopper of a EX6 extrusion line (Filabot, VA) where a single screw with four set heat zones of 60, 190, 195, and 195 °C was used. The molten polymer was extruded into a filament 1.75 mm die head, pulled along an Airpath cooling line (Filabot, VA) using a inline measure (Mitutoyo, Japan), and collected on a Filabot spooler. The produced filament of 1.75 mm was then prepared to be utilized for additive manufacturing (AM).

2.3. Additive Manufacturing

All computer designs and.3MF files were produced using Fusion 360 (Autodesk, CA), which were sliced and converted. GCODE files are then ready for printing by the printer-specific software, PrusaSlicer (Prusa Research, Prague, Czech Republic). The additively manufactured electrodes (AMEs) were additive-manufactured using fused filament fabrication (FFF) technology on a Prusa i3 MK3S+ (Prusa Research, Prague, Czech Republic). The lollipop design AMEs were printed using a 0.6 mm nozzle with a temperature of 215 °C, 100% rectilinear infill, 0.15 mm layer height, and print speed of 70 mm s^{-1}. The 7 mm disc AMEs were printed as 100% concentric infill electrodes (Figure S1), with a layer height of 0.1 mm, extrusion width of 0.4 mm, and a nozzle and bed temperature of 215 and 60 °C, respectively. The experimental AM-BIA cell unit was printed using an HP Material Jet Fusion 580 in PA-12 Nylon and vapor-smoothed using an AMT PostPro SF50.

Physiochemical characterization was performed using thermogravimetric analysis (TGA), X-ray photoelectron spectroscopy (XPS), and scanning electron microscopy (SEM); for further details, please see the Supporting Information.

2.4. Electrochemical Characterization

The electrochemical characterization of the bespoke CB/PLA/TTM filament and comparison to the benchmarks (CB/PLA) were performed on an Autolab 100N potentiostat controlled by NOVA 2.1.6 (Utrecht, the Netherlands) using a lollipop design electrode (Ø

https://doi.org/10.1021/acsaenm.3c00345
ACS Appl. Eng. Mater. 2023, 1, 2397−2406

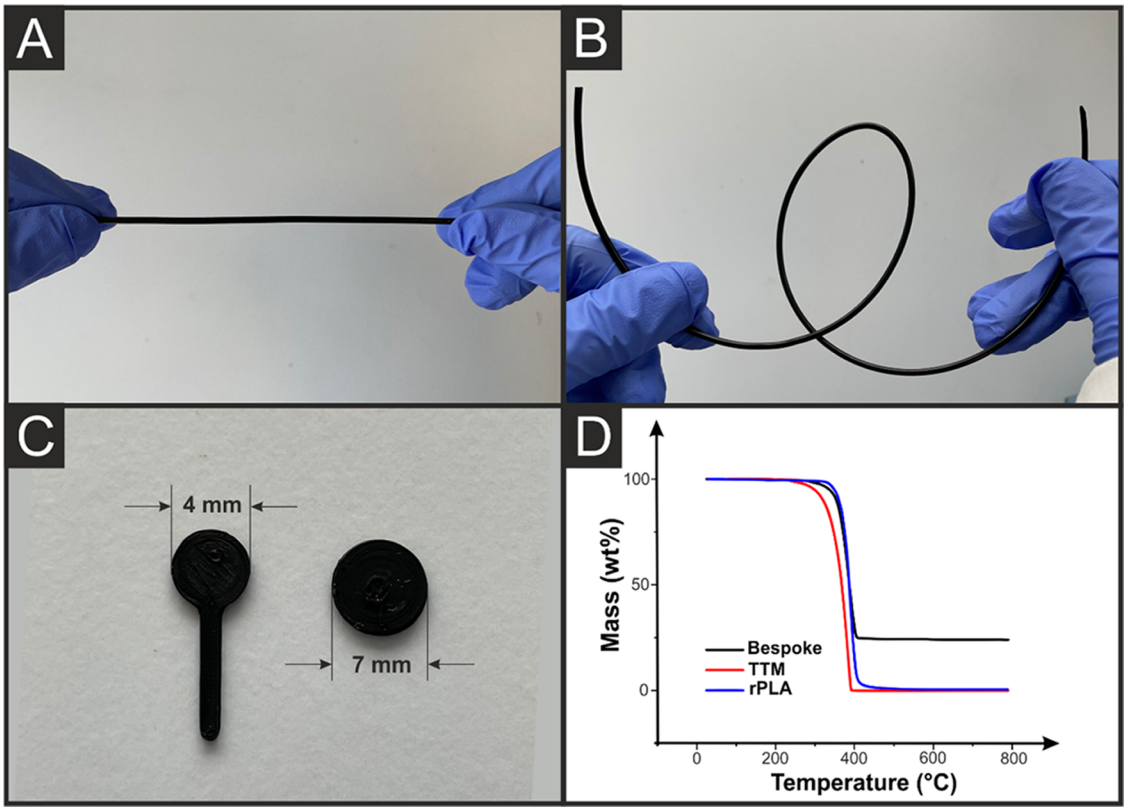

Figure 1. Photographs of (A) straight and (B) bent bespoke CB/PLA/TTM filament, highlighting the flexibility. (C) AMEs in the lollipop and disc designs. (D) Thermal gravimetric analysis of bespoke filament, tris (2-ethylhexyl) trimellitate plasticizer, and recycled PLA.

4, 18 mm connection length, 1 mm thickness) as the working electrode (WE), alongside an external commercial Ag|AgCl reference electrode (RE), and a nichrome wire counter electrode (CE).

Characterizations were done by cyclic voltammetry using $[Ru(NH_3)_6]Cl_3$, ferri/ferrocyanide, and dopamine as probes, and by electrochemical impedance spectroscopy (EIS) with ferri/ferrocyanide. The EIS was recorded at frequencies 10^5 and 10^{-1} s^{-1} at −0.16 V vs Ag|AgCl, with an amplitude of 10 mV. $[Ru(NH_3)_6]Cl_3$ and ferri/ferrocyanide solutions were purged of O_2 thoroughly using N_2 before any electrochemical experiments. The AMEs were electrochemically activated prior to all experiments (except for the $[Ru(NH_3)_6]Cl_3$ measurements) using a well-known procedure by applying +1.4 V followed by −1.0 V (vs Ag|AgCl), both per 200 s in 0.5 mol L^{-1} NaOH solution,[17] unless otherwise described. Atropine initial tests were also performed using the lollipop-shaped AMEs through cyclic voltammetric experiments in the range of 0.0 to +1.2 V (vs Ag|AgCl) at a 50 mV s^{-1} scan rate. The methodology used to establish the heterogeneous electrochemical rate constants, k^0, and the electroactive area of the electrode, A_{real}, are summarized within the Supporting Information.

2.5. Analytical Application

Electrochemical measurements using the flow cell were performed on a Sensit BT PalmSens potentiostat connected to a laptop via USB and controlled by the PSTrace 5.9 software. All three electrodes were additively manufactured using the bespoke filament CB/PLA/TTM, designed in a disc shape (Ø 7, 1 mm thickness) directly connected to the circuit board on the flow cell. The electrodes were submitted to a drop-casting activation with 50 μL of 0.5 mol L^{-1} NaOH solution, which was incubated for 30 min and then rinsed with deionized water.

The proposed AMEs in conjunction with the portable flow cell was evaluated for atropine determination by static analysis using differential pulse voltammetry (DPV) and batch-injection analysis using amperometry (BIA-AMP). DPV measurements were carried out from +0.6 to +1.1 V (vs AME) with a pulse amplitude of 70 mV, a pulse time of 250 ms, and a step potential of 8 mV. BIA-AMP was performed under a +1.1 V (vs AME) applied potential. A Gilson Pipetman (M P200, 20−200 μL) electronic micropipette was used to inject the solutions with a 30 μL s^{-1} dispensing rate and a 15 μL volume. 0.12 mol L^{-1} BR buffer (pH 11) was used as a supporting electrolyte.

Atropine determination was carried out in beverage samples of gin and whisky, which were acquired from local supermarkets. The samples were spiked with 1.5 mmol L^{-1} atropine salt and diluted (100-fold) in the supporting electrolyte.

3. RESULTS AND DISCUSSION

3.1. Fabrication and Characterization of the Recycled Additive Manufactured Filament

The bespoke filament used throughout this work was produced in the same way as seen previously in the literature[10] with the addition of tris(2-ethylhexyl) trimellitate (TTM) as the plasticizer. Including the TTM plasticizer in the filament's composition in a 10% ratio produced a resistance of 835 ± 33 Ω across 10 cm of filament, against 2−3 kΩ quoted for the commercial one.[18] Also, the literature usually reports lab-made brittle filaments with poor printability, contrary to what was obtained with the TTM's presence, ensuring excellent flexibility, as seen in Figure 1A,B. Figure 1C shows the lollipop-shaped AME used for characterizations and the disc electrodes used for the analytical application in the AM-BIA cell.

Thermogravimetric analysis (TGA) of the filament is shown within Figure 1D, with the TTM plasticizer and the recycled PLA (rPLA). Analysis of the pure recycled PLA and the produced filament is critical to understand whether the historical thermal processing of the rPLA and subsequent processing cycles affect the thermal stability of the polymer.

https://doi.org/10.1021/acsaenm.3c00345
ACS Appl. Eng. Mater. 2023, 1, 2397−2406

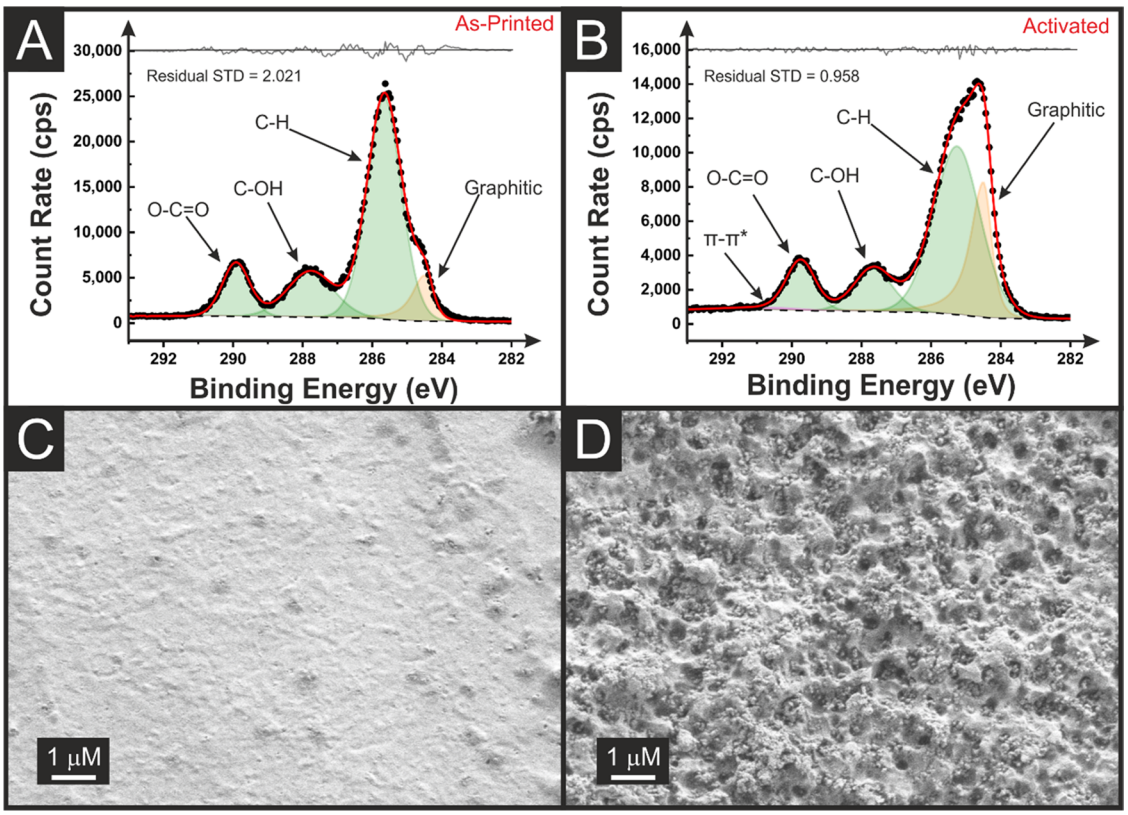

Figure 2. XPS C 1s data for (A) as-printed and (B) activated CB/PLA/TTM electrode, which highlights the increase of the graphitic carbon peak following activation. SEM surface images for (C) as-printed and (D) activated CB/PLA/TTM electrode.

This indicates the effect that the TTM plasticizer has on the stability of the polymer composite and provides accurate information about the mass of the conductive filler present in the bespoke CB/PLA/TTM filament. The average onset temperature obtained for each material was 305 ± 5 °C for rPLA, 210 ± 5 °C for TTM, and 236 ± 6 °C for CB/PLA/TTM. As the onset temperature for pure TTM is significantly lower than that of the pure rPLA, we suggest that the TTM is beginning to degrade at a lower temperature and blends into the degradation of the PLA. Note that the CB filler content for the bespoke filament was calculated at 24 ± 2 wt % by taking the average final mass of the base rPLA away from the final average mass of the bespoke filament, assuming that any nonpolymeric substance that contributes to the remaining rPLA sample mass will also be present in the bespoke filament samples after heating.

XPS was performed to investigate the chemical composition of the bespoke AMEs before and after electrochemical activation in 0.5 M NaOH. Figure 2A,B shows the C 1s spectrum before and after activation, respectively, where an increase in the graphitic carbon peak is exhibited at 284.5 eV from the nonactivated (Figure 2A) to the activated sample (Figure 2B). Additionally, a high binding-energy peak is observed at 290.8 eV for adequately fitting the activated sample, which arises from $\pi-\pi^*$ transitions within the graphitic carbon.[19,20] The presence of this graphitic carbon peak in the activated spectrum provides evidence of the rPLA stripping from the surface and the introduction of CB into the range of XPS.

Further evidence of the exposure of CB after activation is observed through SEM images in Figure 2C,D. Note the nonactivated CB/PLA/TTM electrode; Figure 2C shows evidence of carbon particles covered in a polymeric matrix, which is substantially removed after sample activation, as observed in Figure 2D.

3.2. Electrochemical Characterization of AMEs

After the bespoke filaments had been physically characterized, the electrochemical performance of the electrodes was evaluated. The characterization was performed with lollipop-shaped AMEs as working electrodes, and a nichrome wire and Ag|AgCl were used as the counter and reference electrodes, respectively. Initially, nonactivated AMEs were submitted to *a* cyclic voltammetry scan rate study using the near-ideal outer-sphere redox probe ($[Ru(NH_3)_6]Cl_3$) as shown within Figure 3A,[21] allowing the determination of the heterogeneous electron transfer constant (k^0_{obs}), and the real electrochemical surface area (A_{real}). This is a more accurate representation than the geometric surface area due to the computer design of the stratified printing process and unknown surface roughness of the material. These findings are summarized in Table 1, along with the cathodic peak current ($-I_p^c$) and peak-to-peak separation (ΔE_p) extracted from the 50 mV s^{-1} cyclic voltammograms. When comparing the bespoke AMEs with a commercial filament, the results show a substantial decrease in ΔE_p and an increase in the calculated k^0_{obs} and A_{real}, indicating that introducing TTM in the filament production produces AMEs with an improved electrochemical performance regarding this outer-sphere probe. We used the inner-sphere probe ferri/ferrocyanide, for both commercial and bespoke-activated AMEs. The 50 mV s^{-1} cyclic voltammogram (Figure 3B) also indicates a narrowing in peak potentials, from 611 ± 70 to 232 ± 24 mV, and an increase of ∼2 times in the anodic peak current.

https://doi.org/10.1021/acsaenm.3c00345
ACS Appl. Eng. Mater. 2023, 1, 2397−2406

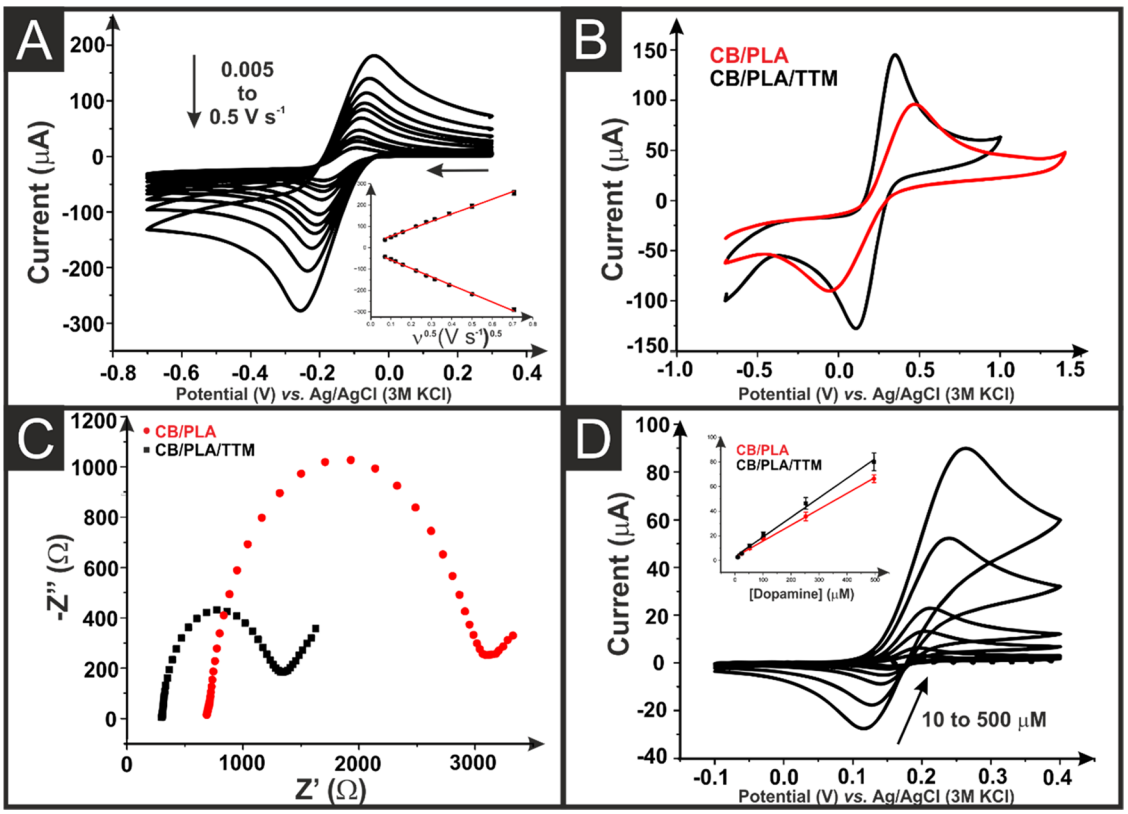

Figure 3. (A) Cyclic voltammograms (5−500 mV s^{-1}) of $[Ru(NH_3)_6]Cl_3$ 1 mM in 0.1 M KCl with CB/PLA/TTM as the WE, nichrome coil CE, and AgIAgCl as RE. The Randles−Ševčík plot is presented. (B) Comparison of the cyclic voltammograms (50 mV s^{-1}) of ferri/ferrocyanide (1 mM in 0.1 M KCl) for CB/PLA/TTM and commercial CB/PLA. (C) Nyquist plot of ferri/ferrocyanide (1 mM in 0.1 M KCl), performed in CB/PLA/TTM and the commercial CB/PLA. (D) Electroanalytical detection of dopamine (10, 25, 50, 100, 250, and 500 μM in 0.01 M PBS, pH 7.4) in CB/PLA/TTM using cyclic voltammograms (50 mV s^{-1}) and the respective calibration curve in comparison with the commercial CB/PLA (inset).

Table 1. Comparisons of the Cathodic Peak Currents ($-I_p^c$), Peak-to-Peak Separations (ΔE_p), Heterogeneous Electron Transfer Constant (k^0_{obs}), Electrochemically Active Area (A_{real}), and EIS Charge Transfer Resistance (R_{ct}) for the Commercial CB/PLA and Proposed CB/PLA/TTM Electrodes

parameter	CB/PLA	CB/PLA/TTM
$-I_p^c$ (μA)[a]	84.9 ± 5.1	107.2 ± 1.8
ΔE_p (mV)[a]	292 ± 7	121 ± 3
k^0_{obs} (cm s^{-1})[b]	(0.30 ± 0.03) × 10^{-3}	(1.85 ± 0.07) × 10^{-3}
A_{real} (cm^2)[b]	0.47 ± 0.02	0.60 ± 0.01
R_{ct} (Ω)[c]	2842 ± 458	995 ± 19
R_s (Ω)[c]	768 ± 96	258 ± 57
sensitivity (μA μM^{-1})[d]	0.1291 ± 0.0027	0.1589 ± 0.0057

[a]Extracted from 50 mV s^{-1} cyclic voltammogram of $[Ru(NH_3)_6]Cl_3$ (1 mM in 0.1 M KCl). [b]Calculated from the $[Ru(NH_3)_6]Cl_3$ scan rate study (5−500 mV s^{-1}). [c]Extracted from Nyquist plots of EIS experiments in a solution of ferri/ferrocyanide (1 mM in 0.1 M KCl). [d]Extracted from calibration plots of dopamine cyclic voltammograms in different concentrations (10−500 μmol L^{-1} in 0.1 M PBS pH 7.4).

EIS experiments in Figure 3C show a large decrease in the parable of the Nyquist plot for CB/PLA/TTM concerning the commercial CB/PLA electrode. The charge transfer resistance (R_{ct}) value for the commercial electrode was estimated at 2842 ± 458 Ω, whereas the bespoke electrode presented a much smaller one (995 ± 19 Ω). Furthermore, the bespoke AME produced a solution resistance (R_s) value of 258 ± 57 Ω in comparison to 768 ± 96 Ω for the commercial electrode, indicating a higher resistance was introduced to the system by the CB/PLA working electrode, as the solution and the other electrochemical equipment are identical. Overall, these results highlight the improved performance of CB/PLA/TTM electrodes.

The calibration plots for dopamine using the bespoke AME and the commercial one are depicted in Figure 3D as insets, with examples of the bespoke electrode cyclic voltammograms in the main figure. The sensitivity of the proposed electrode (0.1589 ± 0.0057 μA μM^{-1}) proved to be slightly higher than that of the commercial electrode (0.1291 ± 0.0027 μA μM), indicating promising features for electroanalytical applications.

3.3. Portable AM-BIA Cell Design

After carrying out all of the characterizations involving the bespoke filament and the AMEs, a suitable electroanalytical sensing platform was designed. Thus, a portable additively manufactured batch-injection analysis (AM-BIA) cell was designed. The portable AM-BIA cell design began with an orthographic scan of the existing PalmSens Sensit BT potentiostat. These scans were then contrast-enhanced and scaled using Adobe Photoshop and Autodesk Fusion 360, to get a profile shape of the mating surfaces of the potentiostat, position of the screw terminals, and overall form-factor of the device (Figure S2). Fusion 360 allows the design of electronics (Figure S3) to be conducted in conjunction with the three-dimensional (3D) modeling of the electronics enclosure itself. Thus, the printed circuit board (PCB) design was led by the positioning of a 2.54 mm pitch pin header component, placed

https://doi.org/10.1021/acsaenm.3c00345
ACS Appl. Eng. Mater. 2023, 1, 2397−2406

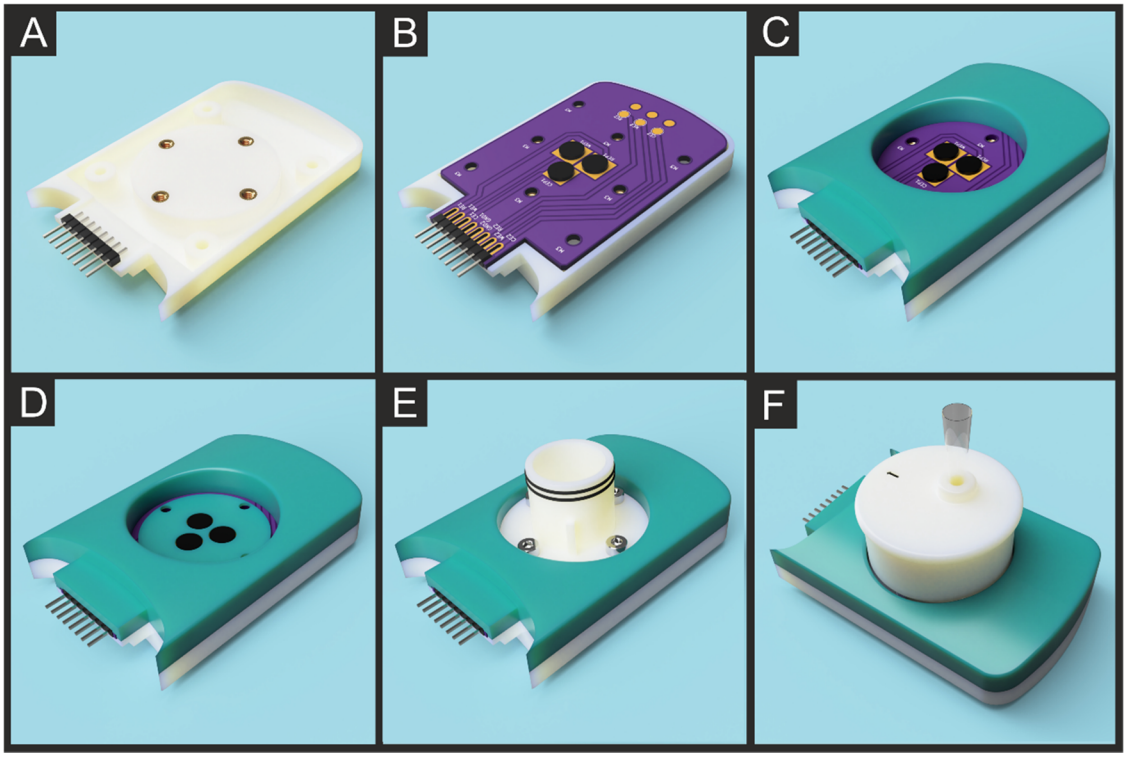

Figure 4. (A) Bottom shell of cell with mounting holes and connector pins. (B) Bottom shell with PCB model imported, and disc AMEs centered on pads. (C) Top shell created. (D) Electrode retainer/separator added. (E) Cell body with lid O-rings added. (F) Completed cell assembly with a pipette tip.

in accordance with manual measurements and the orthographic scan of the end connector, for the two devices to interconnect seamlessly. The housing was created simultaneously around these pins to support the connection and to allow the disassembly of the working components of the device without exposing any mechanical fasteners to chemicals.

Large conductive pads in the center of the PCB were used as WE, CE, and RE connectors. The electrical connection to the disc electrodes is simply made using pressure applied from the cell body, which also creates an O-ring seal between the cell body and disc electrodes, isolating identical surface areas on each electrode (Ø 3 mm). The disc electrodes for this sensing platform were made from the recycled bespoke conductive filament with a material cost of £0.08 per electrode. AM RE and CEs were used in this design as they produce a more user-friendly and lower cost option to commercial electrodes used in the characterization section. Using AM REs in particular causes a shift in peak potentials compared to commercial REs, but they have been shown to be stable.[8] Standard through-hole pads were broken out from every connection in the potentiostat, increasing the usefulness of the device by allowing external modification of the connections. Both channels of the potentiostat have connections for WE, CE, and RE, allowing solder connections to any kind of device/connector or electrode setup the researcher desires, or alternatively bridging connections for different electrochemical techniques that may be needed. Simple modification of the AM housing would allow for any method required.

Figure 4 illustrates the housing design process. Threaded heat-set inserts (highlighted in Figure 4A) were used throughout the design, as clamping force is critical to the experimental procedure. These brass inserts are melted into the AM polymer, creating a hard-wearing and uniformly strong mechanical fixing between AM parts. The PCB is held in place using the four outer holes (Figure 4B), and these holes also serve to fix the top and bottom halves of the device together (Figure 4C), simplifying the overall construction and minimizing the hardware costs. After first prototypes were evaluated, the design was modified slightly to include an "electrode retainer" (Figure 4D) to hold the disc electrodes in the exact position required, while the researcher clamps the cell down onto the electrodes. Figure 4E shows the cell body attached to the device. The cell was designed to hold up to 5 mL of solution. A lid was designed as such that it would hold a pipette tip exactly 2 mm above the working electrode's surface, as is standard in the BIA literature,[22] as seen in Figure 4F. A cross-sectional view (Figure S4) illustrates this. This lid is sealed using nitrile O-rings to prevent spills and accidental contamination of the sample and also serves to prevent light from reaching the sample in case of UV/light-sensitive reagents. The cell's versatile design allows static or flow analysis to be performed by simply removing or adding the lid. PA-12 Nylon used to fabricate the AM-BIA cell produced a highly accurate, smooth, and nonporous surface finish that requires no further post-processing. These AM technologies were chosen due to the high parts accuracy (0.08 mm), and ease of cleaning for practical use. Standard FFF technology is perfectly suited for this use; however, when printed in Prusament PLA on a Prusa i3Mk3s+, it would cost £2.28 in material (Figure S5).

3.4. Analytical Application

3.4.1. Atropine Detection. A portable AM-BIA cell was utilized for the determination of atropine in spiked drink samples using both differential pulse voltammetry (DPV) and

https://doi.org/10.1021/acsaenm.3c00345
ACS Appl. Eng. Mater. 2023, 1, 2397−2406

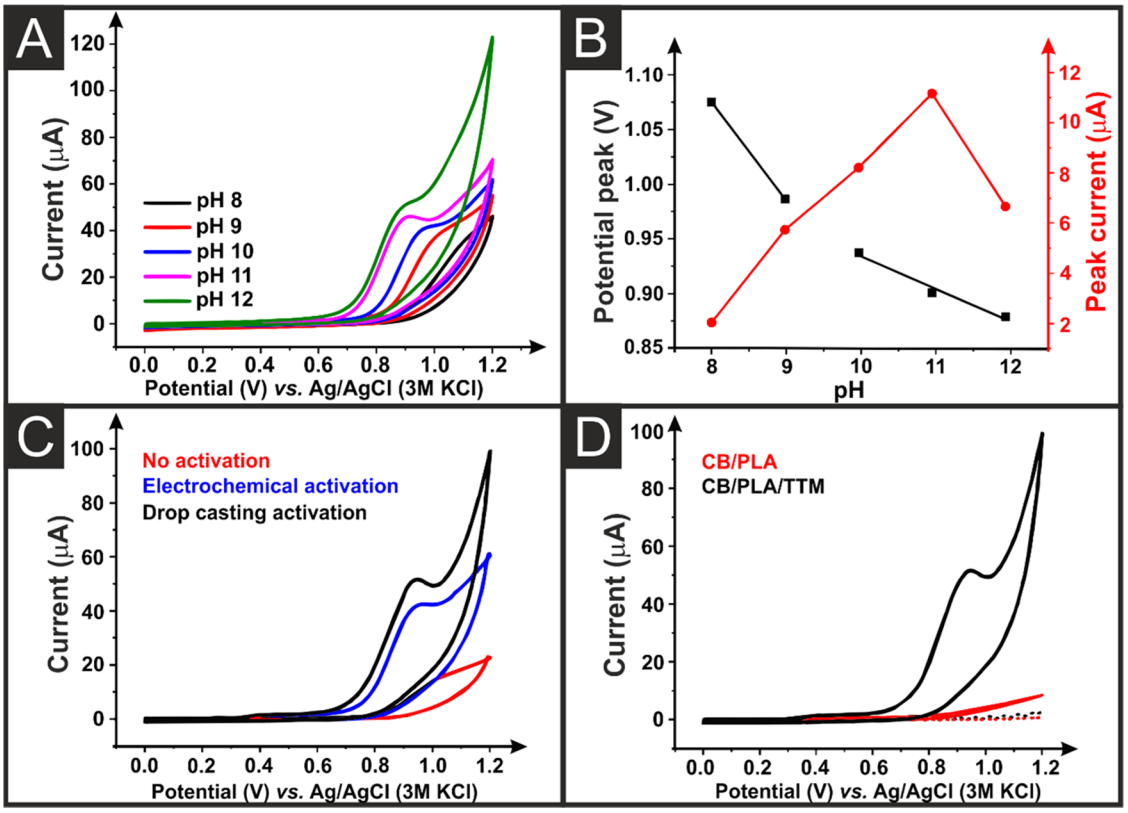

Figure 5. (A) Cyclic voltammogram (50 mV s^{-1}) of 100 μM atropine in 0.12 M BR buffer with different pH values recorded at CB/PLA/TTM as the WE, nichrome coil CE, and AglAgCl as RE. (B) Relation between pH and both peak potential (black) and peak current (red) of atropine oxidation. (C) cyclic voltammogram (50 mV s^{-1}) of 100 μM atropine (0.12 M BR buffer pH 11) with the nonactivated (red) and activated CB/PLA/TTM, both electrochemical (blue) and drop-casting (black) activations using 0.5 M NaOH. (D) Comparison of the cyclic voltammograms (50 mV s^{-1}) of 100 μM atropine (0.12 M BR buffer pH 11) in CB/PLA/TTM and the commercial CB/PLA both activated by drop-casting of 0.5 M NaOH solution.

amperometry (AMP) techniques for static and hydrodynamic analyses, respectively.

Atropine detection was first optimized using cyclic voltammetry to check the behavior at different pH values using 0.12 M BR buffer (Figure 5A). Anodic peaks at around +0.9 V were recorded from pH 8, attributed to the irreversible oxidation of atropine. A shift to less positive potential values is observed with increasing pH, and the largest peak current was observed at pH 11 (Figure 5B), which was chosen for further measurements. Note that in the plot of potential vs pH, there are two linear ranges due to the pK_a of atropine being 9.85. The plot from 10−12 has a gradient of 33 mV pH^{-1}, which agrees with that predicated theoretically (29.5 mV pH^{-1}) and confirms that the mechanism operates via two electrons and one proton. Scheme S1 overviews the electrochemical mechanism of atropine.

Figure 5C shows cyclic voltammetric responses of 100 μM atropine using activated and nonactivated AMEs printed from the bespoke filament. Two types of activation were studied, i.e., the conventional electrochemical activation and a drop-casting procedure, both using 0.5 M NaOH solution, as described in Section 2. As seen, the drop-casting activation provided a comparable current response (15.8 μA) with the electrochemical activation (13.3 μA), presenting a more defined peak, and then it was applied for subsequent analyses, considering the ease of activating the disc electrodes in the final AM-BIA cell assembly.

Under the optimal conditions for atropine detection mentioned above, a comparison with the commercial AME was performed, Figure 5D, demonstrating that CB/PLA itself could not detect the analyte, reinforcing the need for the bespoke CB/PLA/TTM filament.

3.4.2. DPV vs BIA-AMP. The AM-BIA cell was first tested in the static mode by using DPV. Figure S6 shows the optimizations for this technique. Under the optimized conditions, atropine exhibited a linear response from 5 to 100 μM[1] (Figure 6A). The calibration plot shows a good correlation (R = 0.9940) between the peak currents with the concentration (Figure 6B), following the equation I_p (μA) = 0.0148 [Atropine] (μM) + 0.0072. Limits of detection (LOD) and quantification (LOQ) were calculated through the 3σ and 10σ methodologies, resulting in values of 2.60 and 8.80 μM, respectively.

Next, by placing the lid on the cell, the system was tested in hydrodynamic conditions using BIA-AMP. A study of the atropine's amperometric detection potential was carried out, as shown in Figure S7. No satisfactory current signal was detected for applied potentials below +0.9 V; therefore, +1.1 V was fixed for analyte detection as it presented a high current value with a low standard deviation. Intrinsic BIA parameters such as the dispensing rate (Figure S8A) and injection volume (Figure S8B) were also optimized accordingly. Figure 6C shows the linear amperometric response obtained by triplicate injections of atropine solutions into the AM-BIA system. The respective calibration plot (Figure 6D) shows good linearity (R =

https://doi.org/10.1021/acsaenm.3c00345
ACS Appl. Eng. Mater. 2023, 1, 2397−2406

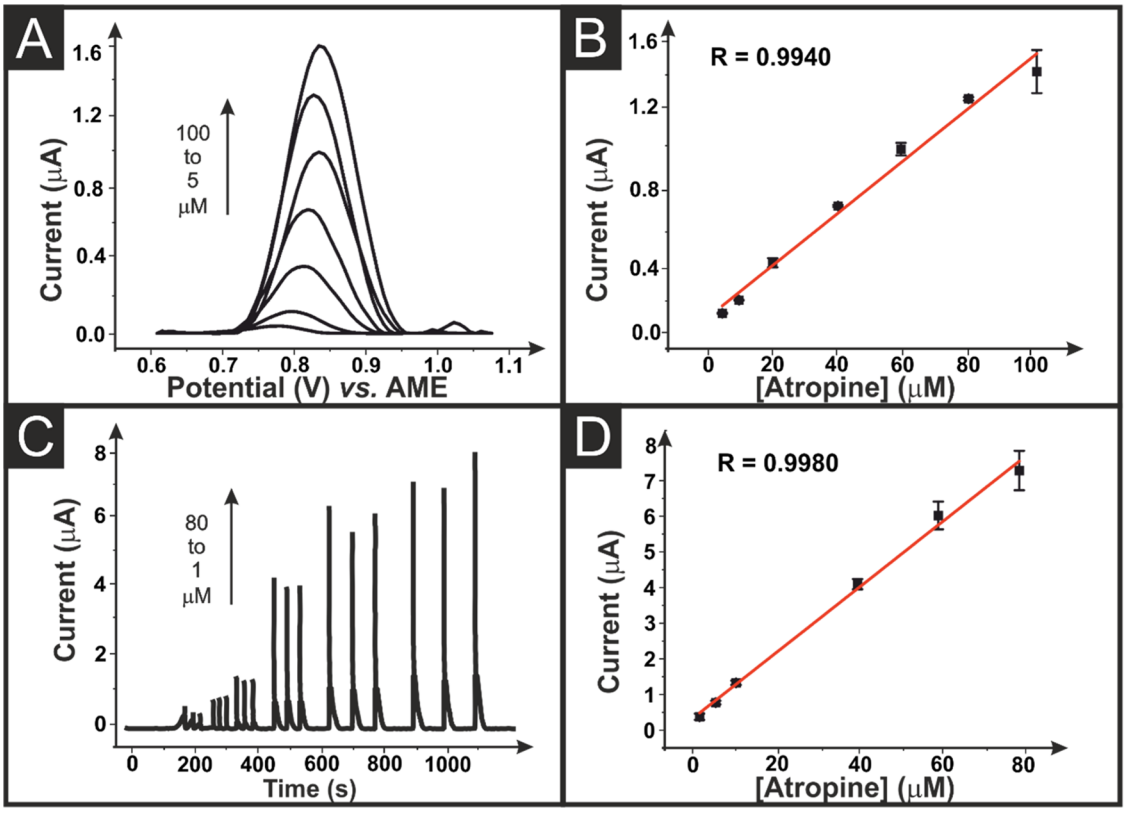

Figure 6. (A) DPV measurements for increasing concentrations of atropine (5−100 μM) in 0.12 M BR buffer pH = 11 and (B) respective calibration curve. Amplitude: 70 mV. Step potential: 8 mV. Modulation time: 250 ms. (C) Amperometric measurements for increasing concentrations of atropine (1−80 μM) in 0.12 mol L^{-1} BR buffer pH = 11 and (D) respective calibration curve. Applied potential: +1.1 V. Injected volume: 15 μL. Dispensing rate: 30 μL s^{-1}.

0.9980), following the equation: I_p (μA) = 0.0783 [Atropine] (μM) + 0.4179. LOD and LOQ values were estimated at 0.51 and 1.68 μM, respectively.

Repeatability tests, Figure S9, were conducted with both methods by measuring/injecting 20 μM atropine solution into the optimized system. Relative standard deviation (RSD) values of 5.7 and 5.6% (n = 20) were obtained for DPV and BIA-AMP, respectively. Additionally, the sample throughput for the hydrodynamic method was estimated at 168 injections per hour, which can be considered satisfactory regarding the conventional BIA literature,[14] especially considering it is a miniaturized system without stirring.

Table 2 compares the analytical parameters obtained using the AM-BIA cell for both methods. Higher sensitivity and lower LOD and LOQ values were obtained by BIA-AMP since there is direct contact between the injected solution and the working electrode, promoting an increase in the analytical signal compared to the static mode. On the other hand, a shorter linear range was observed for the hydrodynamic mode. We assume the system's dispersion is insufficient for concentrations above 80 μM of the analyte, a critical point where stirring is probably needed. For this reason, the system's versatility in performing static and hydrodynamic analyses is so relevant as it is possible to overcome the limitations of one technique using the other when necessary.

Table 2. Comparison of the Analytical Parameters Obtained from Both Methods for Atropine Determination

	DPV	BIA-AMP
linear range (μM)	5−100	1−80
R	0.9940	0.9980
sensitivity (μA M^{-1})	0.0148	0.0783
LOD (μM)	2.60	0.51
LOQ (μM)	8.80	1.68
RSD (%)	5.7	5.6
sample throughput (h^{-1})	n/a	168

Comparing our results with the literature (Table S1) regarding electrochemical atropine detection, we notice similar results with another AME composed of graphene/PLA,[3] with lower LOD presented by our BIA-AMP method. Ensafi et al.[23] reported a LOD value as low as 0.03 mmol L^{-1} using the DPV method for a pencil graphite electrode. However, the electrodes undergo a series of modification steps, whereas our additive manufacturing CB/PLA/TTM electrode requires only an activation step, as simple as drop-casting a NaOH solution to the AMEs.

3.4.3. Real Sample Analysis. The applicability of the bespoke filament fully assembled with the portable AM-BIA cell was assessed through atropine determination in spiked drink samples of gin and whisky. Since atropine has a bitter taste, it can be easily added to these drinks for criminal purposes, especially in party and bar environments.[2] Therefore, accurate in-field analysis would provide greater effectiveness in police decision-making. For this purpose, 10 mL of drink samples were spiked with 10.4 mg of atropine (1.5 mmol L^{-1}), corresponding to the average fatal dose reported in the literature for this drug.[3] The spiked samples were then diluted 100-fold in the supporting electrolyte. The standard addition

https://doi.org/10.1021/acsaenm.3c00345
ACS Appl. Eng. Mater. 2023, 1, 2397−2406

method was used for DPV measurements (Figure S10), while external calibration was performed for the BIA-AMP (Figure S11). Recovery results (from 102 ± 3 to 109 ± 6%) are presented in Table 3, showing good accuracy and absence of samples matrix interference for both methods.

Table 3. Recovery Results Obtained from Both Methods for Beverage Samples Spiked with Atropine

technique	sample	spiked (μmol L^{-1})	found (μmol L^{-1})	recovery (%)
DPV	gin	15	15.7 ± 0.8	103 ± 5
	whisky		16.8 ± 1.0	109 ± 6
BIA-AMP	gin		15.5 ± 0.4	102 ± 3
	whisky		16.6 ± 1.0	107 ± 6

4. CONCLUSIONS

Herein, we demonstrated the fabrication of a portable additively manufactured batch-injection analysis (AM-BIA) cell and 3D-printed electrodes made from a bespoke conductive filament at a £2.53 cost of printable materials. The filament comprises carbon black, recycled PLA, and tris (2-ethylhexyl) trimellitate as a plasticizing agent (CB/PLA/TTM). The addition of the plasticizer provided more flexibility and printability to the filament even with higher loadings of carbon black, giving improved electrochemical features to the manufactured electrodes, such as increased peak currents, reduced ΔE_p, improved k^0_{obs} as well as R_{ct}, and higher electroactive area, compared to the commercially available filament (CB/PLA), as observed through experiments with outer- and inner-sphere redox probes. These electrodes were fully coupled to the AM-BIA cell in a portable electrochemical apparatus, enabling field analysis to detect atropine in spiked drink samples. Compared to a conventional BIA cell, the cell's miniaturized design (~5 mL solution capacity) requires less reagent expense, generating less waste disposal while still maintaining the analytical performance of the system (less than 6% RSD and 168 h^{-1} sample throughput). In addition, the manufactured AM-BIA cell's versatility allows for performing static and hydrodynamic analyses, which were performed using DPV and BIA-AMP techniques. Good analytical parameters were obtained for both methods regarding atropine detection, comparable with the existing literature. Despite DPV allowing a wider linear range detection, BIA-AMP presented higher sensitivity and lower LOD/LOQ values. This shows that different methods can be used depending on the application's needs. Finally, real samples of spiked gin and whisky beverages were analyzed by the two methods in the developed AM system, resulting in recoveries ranging from 102 to 109%, attesting to its applicability for atropine quantification in real forensic scenarios.

ASSOCIATED CONTENT

Supporting Information

The Supporting Information is available free of charge at https://pubs.acs.org/doi/10.1021/acsaenm.3c00345.

Physiochemical characterization, methods to determine the heterogeneous electrochemical rate constants, k^0, and the electroactive area of the electrode, A_{real}, slicer images, potentiostat dimensions, PCB design, AM cell design and slicer images (Section 1); DPV optimization (Section 2); BIA optimizations (Section 3); repeatability tests (Section 4); comparison table (Section 5); DPV real sample analysis (Section 6), and BIA real sample analysis (Section 7) (PDF)

AUTHOR INFORMATION

Corresponding Author

Craig E. Banks − *Faculty of Science and Engineering, Manchester Metropolitan University, Manchester M1 5GD, U.K.;* orcid.org/0000-0002-0756-9764; Phone: +44(0) 1612471196; Email: c.banks@mmu.ac.uk

Authors

Iana V. S. Arantes − *Faculty of Science and Engineering, Manchester Metropolitan University, Manchester M1 5GD, U.K.; Departmento de Química Fundamental, Instituto de Química, Universidade de São Paulo, São Paulo, SP 05508-000, Brazil*

Robert D. Crapnell − *Faculty of Science and Engineering, Manchester Metropolitan University, Manchester M1 5GD, U.K.*

Matthew J. Whittingham − *Faculty of Science and Engineering, Manchester Metropolitan University, Manchester M1 5GD, U.K.*

Evelyn Sigley − *Faculty of Science and Engineering, Manchester Metropolitan University, Manchester M1 5GD, U.K.*

Thiago R.L.C. Paixão − *Departmento de Química Fundamental, Instituto de Química, Universidade de São Paulo, São Paulo, SP 05508-000, Brazil;* orcid.org/0000-0003-0375-4513

Complete contact information is available at: https://pubs.acs.org/10.1021/acsaenm.3c00345

Notes

The authors declare no competing financial interest.

ACKNOWLEDGMENTS

This research was supported by the São Paulo Research Foundation (FAPESP) (Grant numbers 2018/08782-1, 2019/15065-7, and 2022/07552-8) and (CNPq) (Grant number 302839/2020-8). This study was financed in part by the Coordenação de Aperfeiçoamento de Pessoal de Nível Superior—Brasil (CAPES)—Finance Code 001. The authors thank Dr Hayley Andrews and Dr Gary Miller for collecting SEM and XPS data, respectively.

REFERENCES

(1) Ramdani, O.; Metters, J. P.; Figueiredo-Filho, L. C. S.; Fatibello-Filho, O.; Banks, C. E. Forensic electrochemistry: sensing the molecule of murder atropine. *Analyst* **2013**, *138*, 1053−1059.

(2) Crapnell, R. D.; Banks, C. E. Electroanalytical overview: The detection of the molecule of murder atropine. *Talanta Open* **2021**, *4*, No. 100073.

(3) João, A. F.; Rocha, R. G.; Matias, T. A.; Richter, E. M.; Flávio, S.; Petruci, J.; Muñoz, R. A. A. 3D-printing in forensic electrochemistry: Atropine determination in beverages using an additively manufactured graphene-polylactic acid electrode. *Microchem. J.* **2021**, *167*, No. 106324.

(4) Ameen, F.; Hamidian, Y.; Mostafazadeh, R.; Darabi, R.; Erk, N.; Islam, M. A.; Orfali, R. A novel atropine electrochemical sensor based on silver nano particle-coated Spirulina platensis multicellular blue-green microalga. *Chemosphere* **2023**, *324*, No. 138180.

(5) Dushna, O.; Dubenska, L.; Vojs, M.; Marton, M.; Patsay, I.; Ivakh, S.; Plotycya, S. Highly sensitive determination of atropine in pharmaceuticals, biological fluids and beverage on planar electrochemical cell with working boron-doped diamond electrode. *Electrochim. Acta* **2022**, *432*, No. 141182.
(6) Tavana, T.; Rezvani, A. R. Monitoring of atropine anticholinergic drug using voltammetric sensor amplified with NiO@ Pt/SWCNTs and ionic liquid. *Chemosphere* **2022**, *289*, No. 133114.
(7) Cardoso, R. M.; Kalinke, C.; Rocha, R. G.; Dos Santos, P. L.; Rocha, D. P.; Oliveira, P. R.; Janegitz, B. C.; Bonacin, J. A.; Richter, E. M.; Munoz, R. A. Additive-manufactured (3D-printed) electrochemical sensors: A critical review. *Anal. Chim. Acta* **2020**, *1118*, 73−91.
(8) Crapnell, R. D.; Bernalte, E.; Ferrari, A. G.-M.; Whittingham, M. J.; Williams, R. J.; Hurst, N. J.; Banks, C. E. All-in-One Single-Print Additively Manufactured Electroanalytical Sensing Platforms. *ACS Meas. Sci. Au* **2022**, *2*, 167−176.
(9) Ferrari, A. G.-M.; Hurst, N. J.; Bernalte, E.; Crapnell, R. D.; Whittingham, M. J.; Brownson, D. A.; Banks, C. E. Exploration of defined 2-dimensional working electrode shapes through additive manufacturing. *Analyst* **2022**, *147*, 5121−5129.
(10) Sigley, E.; Kalinke, C.; Crapnell, R. D.; Whittingham, M. J.; Williams, R. J.; Keefe, E. M.; Janegitz, B. C.; Bonacin, J. A.; Banks, C. E. Circular economy electrochemistry: creating additive manufacturing feedstocks for caffeine detection from post-industrial coffee pod waste. *ACS Sustainable Chem. Eng.* **2023**, *11*, 2978−2988.
(11) Wuamprakhon, P.; Crapnell, R. D.; Sigley, E.; Hurst, N. J.; Williams, R. J.; Sawangphruk, M.; Keefe, E. M.; Banks, C. E. Recycled Additive Manufacturing Feedstocks for Fabricating High Voltage, Low-Cost Aqueous Supercapacitors. *Adv. Sustainable Syst.* **2023**, *7*, No. 2200407.
(12) Cardoso, R. M.; Mendonça, D. M.; Silva, W. P.; Silva, M. N.; Nossol, E.; da Silva, R. A.; Richter, E. M.; Muñoz, R. A. 3D printing for electroanalysis: From multiuse electrochemical cells to sensors. *Anal. Chim. Acta* **2018**, *1033*, 49−57.
(13) Quintino, M. S.; Angnes, L. Batch injection analysis: An almost unexplored powerful tool. *Electroanalysis* **2004**, *16*, 513−523.
(14) Rocha, D. P.; Cardoso, R. M.; Tormin, T. F.; de Araujo, W. R.; Munoz, R. A.; Richter, E. M.; Angnes, L. Batch-injection Analysis Better than ever: New Materials for Improved Electrochemical Detection and On-site Applications. *Electroanalysis* **2018**, *30*, 1386−1399.
(15) João, A. F.; de Faria, L. V.; Ramos, D. L.; Rocha, R. G.; Richter, E. M.; Muñoz, R. A. 3D-printed carbon black/polylactic acid electrochemical sensor combined with batch injection analysis: A cost-effective and portable tool for naproxen sensing. *Microchem. J.* **2022**, *180*, No. 107565.
(16) Lopes, C. E.; de Faria, L. V.; Araújo, D. A.; Richter, E. M.; Paixão, T. R.; Dantas, L. M.; Muñoz, R. A.; da Silva, I. S. Lab-made 3D-printed electrochemical sensors for tetracycline determination. *Talanta* **2023**, *259*, No. 124536.
(17) Richter, E. M.; Rocha, D. P.; Cardoso, R. M.; Keefe, E. M.; Foster, C. W.; Munoz, R. A.; Banks, C. E. Complete additively manufactured (3D-printed) electrochemical sensing platform. *Anal. Chem.* **2019**, *91*, 12844−12851.
(18) Proto-pasta Composite Conductive Fiber PLA (CDP1xxxx), 2022. https://cdn.shopify.com/s/files/1/0717/9095/files/CDP1xxxx_SDS.pdf?1992606272897634343. (accessed August 17, 2022).
(19) Blume, R.; Rosenthal, D.; Tessonnier, J. P.; Li, H.; Knop-Gericke, A.; Schlögl, R. Characterizing graphitic carbon with X-ray photoelectron spectroscopy: a step-by-step approach. *ChemCatChem* **2015**, *7*, 2871−2881.
(20) Gengenbach, T. R.; Major, G. H.; Linford, M. R.; Easton, C. D. Practical guides for x-ray photoelectron spectroscopy (XPS): Interpreting the carbon 1s spectrum. *J. Vac. Sci. Technol., A* **2021**, *39*, No. 013204.
(21) McCreery, R. L. Advanced carbon electrode materials for molecular electrochemistry. *Chem. Rev.* **2008**, *108*, 2646−2687.
(22) Wang, J.; Taha, Z. Batch injection analysis. *Anal. Chem.* **1991**, *63*, 1053−1056.
(23) Ensafi, A. A.; Nasr-Esfahani, P.; Heydari-Bafrooei, E.; Rezaei, B. Determination of atropine sulfate using a novel sensitive DNA−biosensor based on its interaction on a modified pencil graphite electrode. *Talanta* **2015**, *131*, 149−155.

https://doi.org/10.1021/acsaenm.3c00345
ACS Appl. Eng. Mater. 2023, 1, 2397−2406